Analytical small-time asymptotic properties of $A+B\rightarrow C$ fronts

P. M. J. Trevelyan
Nonlinear Physical Chemistry Unit, Center for Nonlinear Phenomena and Complex Systems, Faculté des Sciences, Université Libre de Bruxelles (ULB), CP 231, 1050 Brussels, Belgium

(Received 6 May 2009; revised manuscript received 28 July 2009; published 22 October 2009)

The small-time asymptotic properties of the reaction front formed by a reaction $A+B\rightarrow C$ coupled to diffusion are considered. Reactants A and B are initially separately dissolved in two identical solvents. The solvents are brought into contact and the reactants meet through diffusion. The small-time asymptotic position of the center of mass of the reaction rate is obtained analytically. When one of the reactants diffuses much faster than the other reactant then the position of the local maximum in the reaction rate travels on a length scale related to the diffusion coefficient of the slowest diffusing reactant while the first moment of the reaction rate and the width of the reaction front are on a length scale related to the diffusion coefficient of the fastest diffusing reactant. If the sum of the initial reactant concentrations is fixed, then the fastest reaction rate is obtained when equal concentrations are used. The first-order solutions are analytically obtained, however, each solution involves an integral which requires numerical evaluation. Various small-time asymptotic analytical reaction front properties are obtained. In particular, one finds that the position of the center of mass of the product concentration distribution is initially located at three quarters of the position of the center of mass of the reaction rate.

DOI: 10.1103/PhysRevE.80.046118 PACS number(s): 82.20.Db, 82.20.Wt, 82.40.−g

I. INTRODUCTION

When a chemical reaction changes a fluid's physical properties, e.g., its density, viscosity, or surface tension, then convection can be induced. Some recent theory and experiments on convection induced by chemical reactions have analyzed various hydrodynamic instabilities that can deform reaction-diffusion base states [1–6].

For transient problems in which a system switches from a stable regime to an unstable regime, linear stability analysis is a useful analyzing technique in predicting the onset time of the instability and further the linear stability predictions can remain valid up to the start of the nonlinear regime. When the linear stability analysis employs the quasi-steady state approximation, then the instability of the system is determined using convection-free base-state concentration profiles which are assumed to be frozen in time. Hence, a clear understanding of these base-state profiles can be an essential part in determining the behavior of the instability. Indeed such a situation is the starting point for the identification and evaluation of the onset of an instability [7].

A simple reaction mechanism between two reactants is the scheme $A+B\overset{k}{\rightarrow}C$ in which the production rate $R=k\hat{A}\hat{B}$, where $\hat{A}$ and $\hat{B}$ denote concentrations and k is the kinetic constant. The diffusion limited problem of two initially separated reactants that are brought into contact along a planar interface has received much attention. For large times T, Venzl [8] found that the position of the reaction front, X_f, scales with $T^{1/2}$ when the reactants have equal diffusion coefficients. Further Gálfi and Rácz [9] determined that the reaction zone width $W_f\sim T^{1/6}$ and the rate of production at the front $R\sim T^{-2/3}$. The scalings for the position of the front and width of the reaction zone were found to be in good agreement with results from experiments conducted in gels [10,11]. These results were then generalized by Koza [12] for arbitrary diffusion coefficients, with the large time scalings found to be unaffected. Sinder and Pelleg [13] obtained the solution for the product for both reversible and irreversible reactions. By using the reaction $nA+mB\rightarrow C$, Cornell *et al.* [14–16] found that although the reaction front position and total reaction rate still scaled with $\sqrt{T}$ and $T^{-1/2}$, respectively, the reaction rate at the front and the width of the reaction rate now scaled with $T^{-2\sigma}$ and $T^{1/2-\sigma}$, respectively, where $\sigma=1/(n+m+1)$. The properties of such a reaction front in immiscible liquids were recently examined by Trevelyan *et al.* [17] who found that the center of mass of the product could travel in the opposite direction to the reaction front. The first-order correction to the large time asymptotic solution for the reaction $nA+mB\rightarrow C$ has furthermore been obtained [18] and it was found that the position of the reaction front could be more accurately described by $X_f\approx 2\sqrt{T}[\alpha+\alpha_2 T^{-2\sigma}]$. This can lead to reaction fronts traveling with different time scalings when the reactants diffuse at different rates and the initial concentration ratio is chosen appropriately.

The small-time asymptotic limit of this problem is not as clearly understood as the large time asymptotic limit. We note that, as this problem has no intrinsic length scale, the small-time asymptotic limit is equivalent to the asymptotically slow reaction rate limit. Taitelbaum *et al.* [19] found that the position and width of the reaction front along with the total rate of production were all found to increase like $\sqrt{T}$ for small times. Further, the first-order correction to the solution in the small-time asymptotic limit was analytically expressed in terms of a double integral using the Green's function for the diffusion equation. The correction to the total rate of the reaction was then found to scale with $T^{3/2}$. Then Taitelbaum *et al.* [20] introduced approximate solutions for the small-time limit and found that the reaction front could change direction under certain conditions upon the initial concentration ratio and the ratio of the diffusion coefficients. Recently similar approximate solutions have been ap-

plied to systems with competing reactions by Hecht and Taitelbaum [21]. The direction of the reaction front was numerically found to actually change direction twice by Taitelbaum and Koza [22].

In this study the small-time asymptotic properties of the reaction front are obtained analytically on the basis of a one-dimensional model of this reaction-diffusion system. In the small-time asymptotic limit the corrections to the zeroth-order solutions are expressed analytically using single integrals with the concentrations and their gradients at the initial interface obtained exactly. The first moment of the reaction rate is found to travel faster than the position of the maximum reaction rate in the small-time asymptotic limit. First-order solutions in time of the reactant concentrations are obtained in the asymptotic limit when one reactant diffuses much faster than the other one. Here we find that the location where the maximum leading order correction to the slowest diffusing reactant and the position where the reaction rate is maximum are related to the smallest reactant diffusion coefficient. However, the location where the maximum leading order correction to the fastest diffusing reactant, the first moment of the reaction rate, and the width of the reaction rate are all related to the largest reactant diffusion coefficient.

A brief summary of the six types of behaviors exhibited by reaction fronts throughout the full course of time is given in Sec. III. The small-time asymptotic equations are listed in Sec. IV. The zeroth-order reaction front properties are presented in Sec. V and the first-order solutions are given in Sec. VI. In Sec. VII various integral measures of the solutions are obtained and show that the position of the center of mass of the product concentration distribution is initially located at three quarters of the position of the center of mass of the reaction rate.

II. PHYSICAL MODEL

Consider two identical solvents placed in contact along a planar interface, $X=0$, at time $T=0$. The solvent on the left, i.e., $X<0$, initially contains reactant A homogeneously distributed at concentration $\hat{A}_0$, while the solvent on the right, i.e., $X>0$, initially contains reactant B homogeneously distributed at concentration $\hat{B}_0$. The reaction scheme is simply $A+B\rightarrow C$. The mean field approximation is assumed and the rate of production is thus given by $R=k\hat{A}\hat{B}$, where k is the kinetic constant and $\hat{A}$ and $\hat{B}$ are the concentrations of A and B, respectively. This problem is modeled using the following system of one-dimensional reaction-diffusion equations:

$$\hat{A}_T = D_a\hat{A}_{XX} - k\hat{A}\hat{B}, \tag{1a}$$

$$\hat{B}_T = D_b\hat{B}_{XX} - k\hat{A}\hat{B}, \tag{1b}$$

$$\hat{C}_T = D_c\hat{D}_{XX} + k\hat{A}\hat{B}, \tag{1c}$$

where $\hat{C}$ denote the concentration of C. The subscripts X and T denote partial derivatives with respect to space and time. The concentrations of the species are considered sufficiently dilute that the molecular diffusion coefficients D_a, D_b, and D_c can be assumed constant.

As this study is concerned with small times the size of the domain can effectively be treated as infinite. Thus, at infinity we apply no flux conditions,

$$\hat{A}_X, \hat{B}_X, \hat{C}_X \rightarrow 0 \quad \text{as} \quad X \rightarrow \pm\infty. \tag{1d}$$

Finally, the initial conditions are

$$\hat{A} = \hat{A}_0, \quad \hat{B} = \hat{C} = 0 \quad \text{for} \quad X < 0, \tag{1e}$$

$$\hat{B} = \hat{B}_0, \quad \hat{A} = \hat{C} = 0 \quad \text{for} \quad X > 0. \tag{1f}$$

To nondimensionalize system (1), the characteristic length and time scales are constructed using the kinetic constant, the initial concentration of reactant A, and the diffusion coefficient of reactant A, i.e.,

$$l_0 = \sqrt{D_a t_0} \quad \text{and} \quad t_0 = \frac{1}{k\hat{A}_0},$$

where the dimensionless variables are $x=X/l_0$, $t=T/t_0$, $a=\hat{A}/\hat{A}_0$, $b=\hat{B}/\hat{A}_0$, and $c=\hat{C}/\hat{A}_0$. The dimensionless parameters introduced are

$$\varphi = \frac{\hat{B}_0}{\hat{A}_0}, \quad r = \sqrt{\frac{D_a}{D_b}}, \quad s = \sqrt{\frac{D_a}{D_c}} \tag{2}$$

with φ representing the initial reactant concentration ratio, while r and s represent the square root of the concentration ratios. The resulting system of equations is

$$a_t = a_{xx} - ab, \quad b_t = \frac{b_{xx}}{r^2} - ab, \quad c_t = \frac{c_{xx}}{s^2} + ab. \tag{3a}$$

The far field conditions are now

$$a_x, b_x, c_x \rightarrow 0 \quad \text{as} \quad x \rightarrow \pm\infty, \tag{3b}$$

while at $t=0$, the initial conditions read

$$a = 1, \quad b = c = 0 \quad \text{for} \quad x < 0, \tag{3c}$$

$$b = \varphi, \quad a = c = 0 \quad \text{for} \quad x > 0. \tag{3d}$$

It is useful to transform the full system of equations from x and t to η and t where

$$\eta = \frac{x}{2\sqrt{t}}. \tag{4}$$

Thus, the transport equations become

$$a_t - \frac{\eta a_\eta}{2t} = \frac{a_{\eta\eta}}{4t} - ab, \tag{5a}$$

$$b_t - \frac{\eta b_\eta}{2t} = \frac{b_{\eta\eta}}{4r^2 t} - ab, \tag{5b}$$

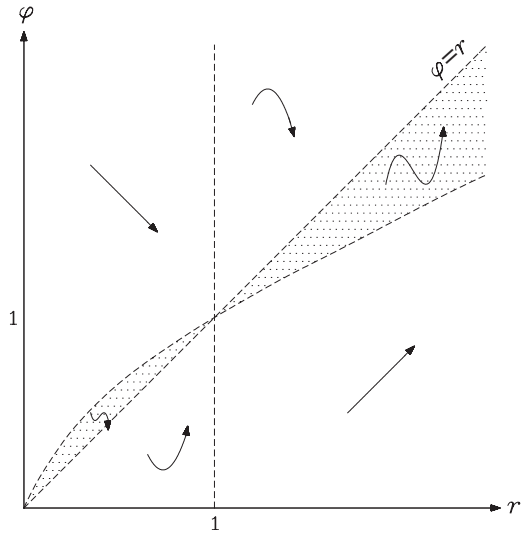

FIG. 1. Dynamics of the reaction front in the six regions of the $r-\varphi$ plane. The shapes of the arrows are sketches of the space-time plot of the reaction front (the first moment of the reaction rate). The initial behavior of the reaction front corresponds to the start of the arrow tail while the large time behavior of the reaction front corresponds to the arrow head. Reaction fronts that eventually propagate in the positive direction have arrows pointing upward. The regions where a reaction front changes direction twice are shaded.

$$c_t - \frac{\eta c_\eta}{2t} = \frac{c_{\eta\eta}}{4s^2 t} + ab. \tag{5c}$$

The initial conditions at $t=0$ for all η are equivalent to the far field conditions as $|\eta| \to \infty$ for all t and are given by

$$a = 1, \quad b = c = 0 \quad \text{for} \quad \eta < 0, \tag{5d}$$

$$b = \varphi, \quad a = c = 0 \quad \text{for} \quad \eta > 0. \tag{5e}$$

This study will focus on the small-time asymptotic properties of dimensionless system (5). Previous slow reaction rate studies on this problem have employed a different nondimensionalization resulting in a three parameter problem for the two reactants [19,20,23], namely, $k/\sqrt{(\hat{A}_0 \hat{B}_0 D_a D_b}$, $\sqrt{D_a/D_b}$, and $\sqrt{\hat{A}_0/\hat{B}_0}$, while here the two reactant problem only depends on the two parameters r and φ. As this study is directed toward applications in time dependent base-state solutions for linear stability analysis, here both reactants and the product are considered. Hence, this problem depends on the three dimensionless parameters given in Eq. (2).

III. SYSTEM DYNAMICS

To set the context of this problem a very brief outline of the behavior of the full dynamics of this system is first presented. By numerically solving system (3) in time one finds that there are six different possible behaviors for the direction of the resulting reaction front (see Fig. 1). Here the reaction front is defined as the first moment of the reaction rate. The path taken by the reaction front is indicated on Fig. 1 by the shape of the arrow tail.

The reaction front is found to initially propagate in the positive direction if and only if $r>1$, i.e., reactant A diffuses faster than reactant B. This result was found by Taitelbaum *et al.* [19] for the position of the maximum of the reaction rate. This is illustrated in Fig. 1 when $r>1$, by the initial part of the arrow tail moving upward. Eventually, for large times, the reaction front is found to propagate in the positive direction if and only if $r>\varphi$, i.e., $\hat{A}_0\sqrt{D_a} > \hat{B}_0\sqrt{D_b}$ which means that the diffusion limited flux of reactant A is greater than the diffusion limited flux of reactant B. This result was determined by Koza [12] [see Eq. (26)]; however, it could have been derived from Eq. (8.1) in [24], which is a generalized version of Eq. (24) in [12]. This is illustrated in Fig. 1 when $r>\varphi$, by the arrow head pointing upward. The shaded regions in Fig. 1 correspond to the situation when the reaction front changes direction twice. This occurs for a region of the parameter space contained inside the domains $r>\varphi>1$ or $r<\varphi<1$, so that the small and large time asymptotic limits predict the same direction for the reaction front, but during moderate times the reaction front travels in the opposite direction. This type of behavior was first identified by Taitelbaum and Koza [22]. The condition for a reaction front to change direction twice will not be addressed by this study as such behavior does not occur in the small-time asymptotic limit. One notes that if the point (r,φ) is on this critical line then so is the point $(1/r, 1/\varphi)$.

IV. SMALL-TIME ASYMPTOTIC EXPANSION

To determine the initial behavior of the reaction front a small-time asymptotic expansion of each variable is carried out by writing

$$\Gamma = \Gamma_0(\eta) + t^\mu \Gamma_1(\eta) + t^{2\mu}\Gamma_2(\eta) + O(t^{3\mu}), \tag{6}$$

where μ is a positive constant and Γ represents the concentrations a, b, and c. Substituting the expansions into system (5) reveals that $\mu=1$ so that the leading order correction terms can balance the reactive term. We collect the equations by equating the coefficients of the powers of t.

The zeroth-order solutions are then given by

$$a_0 = \frac{1}{2}\text{erfc}(\eta), \quad b_0 = \frac{\varphi}{2}\text{erfc}(-r\eta) \tag{7}$$

with $c_0=0$. These correspond to purely diffusive nonreactive solutions [25,26]. The system of first-order transport equations is

$$a_1 - \frac{\eta a_{1\eta}}{2} = \frac{a_{1\eta\eta}}{4} - a_0 b_0, \tag{8a}$$

$$b_1 - \frac{\eta b_{1\eta}}{2} = \frac{b_{1\eta\eta}}{4r^2} - a_0 b_0, \tag{8b}$$

$$c_1 - \frac{\eta c_{1\eta}}{2} = \frac{c_{1\eta\eta}}{4s^2} + a_0 b_0, \tag{8c}$$

whose associated far field conditions are $a_1, b_1, c_1 \to 0$ as $|\eta| \to \infty$. The system of second-order transport equations is

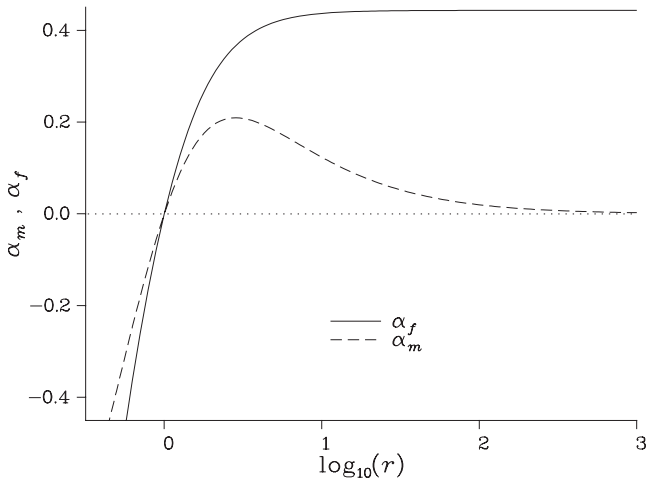

FIG. 2. Comparison of α_f and α_m against $\log_{10}(r)$, where $\alpha_f = x_f/\sqrt{4t}$ and α_m is the solution to Eq. (10).

$$2a_2 - \frac{\eta a_{2\eta}}{2} = \frac{a_{2\eta\eta}}{4} - a_1 b_0 - a_0 b_1, \tag{9a}$$

$$2b_2 - \frac{\eta b_{2\eta}}{2} = \frac{b_{2\eta\eta}}{4r^2} - a_1 b_0 - a_0 b_1, \tag{9b}$$

$$2c_2 - \frac{\eta c_{2\eta}}{2} = \frac{c_{2\eta\eta}}{4s^2} + a_1 b_0 + a_0 b_1, \tag{9c}$$

whose associated far field conditions are $a_2, b_2, c_2 \to 0$ as $|\eta| \to \infty$.

Before examining the corrections to the zeroth-order solutions, first the reaction front properties of the zeroth-order solution are considered.

V. ZEROTH-ORDER REACTION FRONT PROPERTIES

The position of the reaction front is usually described as the point where the reaction rate is maximum or as the first moment of the reaction rate [27]. To distinguish between these definitions, x_m is introduced to denote the position where the reaction rate is maximum and x_f is used to denote the first moment of the reaction rate.

A. Maximum of the reaction rate

In the small-time asymptotic limit Koza [12] was able to obtain $x_m = 2\alpha_m\sqrt{t}$, where α_m satisfies

$$e^{r^2\alpha_m^2}\,\mathrm{erfc}(-r\alpha_m) = re^{\alpha_m^2}\,\mathrm{erfc}(\alpha_m). \tag{10}$$

By numerically solving Eq. (10) for α_m its dependence on the parameter r is illustrated in Fig. 2.

An expansion in small α_m yields the approximation

$$\alpha_m \approx \frac{\sqrt{\pi}(r-1)}{4r},$$

which is valid when $|r-1| \ll 1$, showing that the small-time asymptotic direction of the reaction front is solely dependent on r with $x_m > 0$ if and only if $r > 1$, as was pointed out in [19].

As $r \to 0$, using Eq. (10), one finds that

$$\alpha_m \to -\sqrt{\ln\left(\frac{1}{2r}\right)}, \tag{11}$$

which slowly tends to $-\infty$. In dimensional quantities using $X_m = 2\alpha_m\sqrt{D_a T}$ we find that

$$X_m \to -\sqrt{2D_a T \ln\left(\frac{D_b}{4D_a}\right)}.$$

As one would physically expect, this means that the reaction front moves further to the left and invades the liquid containing reactant A faster as the diffusion coefficient of reactant B tends to infinity. One notes that the position of the local maximum in the limit of $D_b \gg D_a$ has a much stronger dependence on D_a than D_b as expected since the maximum reaction rate would be on the diffusive length scale of reactant A.

As $r \to \infty$, using Eq. (10), one finds that

$$\alpha_m \to \frac{1}{r}\sqrt{\ln\left(\frac{r}{2}\right)}, \tag{12}$$

which slowly tends to 0. Recalling that α_m increases as r increases above 1 and now that α_m decreases as $r \to \infty$ means that there exists a maximum value of α_m. Numerically this maximum is found to occur at $r \simeq 2.8384$ with $\alpha_m \simeq 0.2092$. Although a local maximum in α_m appears unexpected, in fact in dimensional quantities this limit becomes

$$X_m \to \sqrt{2D_b T \ln\left(\frac{D_a}{4D_b}\right)},$$

which, as one would physically expect, means that the reaction front moves further to the right and invades the liquid containing reactant B faster as the diffusion coefficient of reactant A tends to infinity. Thus the local maximum α_m is only related to the dimensionless problem and is not relevant to the physical problem. As a further check one notes that the dimensional limit is consistent with the limit when $r \to 0$ with A and B taking reverse roles.

B. Moments of the reaction rate

The dimensional first moment of the reaction rate is given by

$$X_f = \frac{\int_{-\infty}^{\infty} RX\,dX}{\int_{-\infty}^{\infty} R\,dX},$$

while a measure of the width of the reaction front, W_f, is defined using the second moment of the reaction rate, as

$$W_f^2 = \frac{\int_{-\infty}^{\infty} R(X - X_f)^2 dX}{\int_{-\infty}^{\infty} R dX}.$$

In dimensionless variables with $x_f = X_f / l_0$ and $w_f = W_f / l_0$ and using the definition of η one obtains

$$x_f = 2\sqrt{t}\frac{\int_{-\infty}^{\infty} ab\eta d\eta}{\int_{-\infty}^{\infty} abd\eta}, \quad w_f^2 = 4t\frac{\int_{-\infty}^{\infty} ab\eta^2 d\eta}{\int_{-\infty}^{\infty} abd\eta} - x_f^2.$$

At this point it is useful to define

$$I_\nu = \int_{-\infty}^{\infty} \eta^\nu a_0 b_0 d\eta, \tag{13}$$

where ν is a non-negative integer. The zeroth-order small-time asymptotic position and width of the front are thus given by

$$x_f = 2\sqrt{t}\frac{I_1}{I_0}, \quad w_f^2 = 4t\frac{I_2}{I_0} - x_f^2.$$

Then using the solutions for a_0 and b_0 in Eq. (7) and using the definite integrals in Appendix A one can evaluate I_0 to obtain

$$I_0 = \int_{-\infty}^{\infty} a_0 b_0 d\eta = \frac{\varphi\sqrt{1+r^2}}{2\sqrt{\pi}r}, \tag{14}$$

which means that the small-time asymptotic total production rate $\int_{-\infty}^{\infty} a_0 b_0 dx = 2\sqrt{t} I_0$ scales with $\sqrt{t}$. One notes that I_0 is a positive monotonic decreasing function of r such that $I_0 \geq \frac{\varphi}{2\sqrt{\pi}}$ and tends to infinity as $r \to 0$. In dimensional quantities this yields

$$\int_{-\infty}^{\infty} k\hat{A}\hat{B} dX = \frac{k}{\sqrt{\pi}}\hat{A}_0\hat{B}_0\sqrt{D_a + D_b}\sqrt{T},$$

which one notes is proportional to the square root of the sum of the reactant diffusion coefficients. If one of the diffusion rates tend to infinity so does the total production rate. However, if both of the diffusion coefficients tend to zero, so does the total production rate, as the reactants can only meet through diffusion. In the case when one of the reactant diffusion coefficients is zero the total production rate remains positive. Additionally if one introduces that the constraint $\hat{A}_0 + \hat{B}_0$ is a fixed constant, then the total production rate is maximized, in the small-time asymptotic limit, when $\hat{A}_0 = \hat{B}_0$. If one is using a slow chemical reaction and the costs of both reactants are the same, then this means that the cost of producing species C is minimized when equal amounts of the reactants are used.

One can evaluate I_1 using the definite integrals in Appendix A to obtain

$$I_1 = \int_{-\infty}^{\infty} \eta a_0 b_0 d\eta = \frac{\varphi(r^2 - 1)}{8r^2}. \tag{15}$$

One notes that I_1 is a monotonic increasing function of r such that $I_1 \leq \frac{\varphi}{8}$; it is zero at $r=1$ and tends to minus infinity as $r \to 0$. The zeroth-order first moment of the reaction rate is given by

$$x_f = \frac{\sqrt{\pi t}}{2r}\frac{[r^2 - 1]}{\sqrt{1 + r^2}}. \tag{16}$$

Hence, like x_m, the short time position of the reaction front x_f has been found to depend only on the parameter r with the initial concentration ratio φ playing no part. The reaction front is initially stationary if and only if $r=1$. We notice that although both x_m and x_f scale with $\sqrt{t}$, in general they do not coincide. It should be noted that in a recent paper by Trevelyan [18] in Appendix C, it was incorrect to say that the small-time asymptotic first moment of the reaction rate involves integrals which must be evaluated numerically since Eq. (16) describes this analytically.

Returning to dimensional quantities one obtains

$$X_f = \frac{\sqrt{\pi T}[D_a - D_b]}{2\sqrt{D_a + D_b}}.$$

Again, just like X_m, the small-time asymptotic reaction front position is only stationary when $D_a = D_b$. If one of the diffusion coefficients is zero, say that of reactant B, then one obtains $X_f = \sqrt{\pi D_a T / 4}$. Importantly, we notice that, unlike X_m, if one of the reactants diffuses much faster than the other then X_f scales with the square root of the diffusion coefficient of the fastest diffusing reactant.

In order to compare the positions x_f with x_m it is useful to introduce $\alpha_f = x_f / \sqrt{4t}$. Then plotting α_f and α_m against $\log_{10}(r)$ (see Fig. 2) reveals that $|\alpha_f| > |\alpha_m|$, so that the first moment of the reaction front travels faster than the position of the maximum reaction rate in the small-time asymptotic limit. Further, as $r \to \infty$ we observe that $\alpha_m \to 0$ while $\alpha_f \to \sqrt{\pi}/4$. At this point it is useful to note that if one returns to Fig. 1 based on x_f obtained numerically from solving system (5), we find that the region in the $r - \varphi$ parameter space where the reaction front changes direction twice is slightly different if x_m is considered instead of x_f.

Using the definite integrals in Appendix A, one obtains

$$I_2 = \int_{-\infty}^{\infty} \eta^2 a_0 b_0 d\eta = \varphi\frac{2r^4 + r^2 + 2}{12\sqrt{\pi}r^3\sqrt{r^2 + 1}}. \tag{17}$$

One notes that I_2 is a positive monotonic decreasing function of r such that $I_2 \geq \frac{\varphi}{6\sqrt{\pi}}$ and tends to infinity as $r \to 0$. The small-time asymptotic width of the reaction front is given by

$$w_f^2 = \frac{t}{r^2(r^2+1)}\left[(r^4+1)\left(\frac{4}{3} - \frac{\pi}{4}\right) + r^2\left(\frac{2}{3} + \frac{\pi}{2}\right)\right] \tag{18}$$

so that w_f scales like $\sqrt{t}$. This time scaling was found in [19]. As $r \to 0$, w_f scales with r^{-1}, while as $r \to \infty$, w_f becomes independent of r. In dimensional quantities one obtains

$$W_f^2 = \frac{T}{D_a + D_b}\left[(D_a^2 + D_b^2)\left(\frac{4}{3} - \frac{\pi}{4}\right) + D_a D_b \left(\frac{2}{3} + \frac{\pi}{2}\right)\right],$$

which monotonically increases with both D_a and D_b. One notes that when $D_a = D_b$ then $W_f^2 = \frac{5}{3} T D_a$. If one of the diffusion coefficients is zero, say that of reactant B, then one obtains $W_f^2 = T D_a (\frac{4}{3} - \frac{\pi}{4})$. This shows that the width of the reaction front is linked to the diffusion coefficient of the fastest diffusing reactant.

VI. FIRST-ORDER SOLUTIONS

The first-order expansions for the concentration of species A, B, and C are $a = a_0 + t a_1$, $b = b_0 + t b_1$, and $c = t c_1$. In particular these expansions show that the amount of product present initially increases linearly with time, t. In this section the corrections a_1, b_1, and c_1 are sought.

Taitelbaum *et al.* [19] expressed the solution to a system equivalent to Eq. (5) using a Green's function, however, such a solution is difficult to analyze analytically. Thus, Taitelbaum *et al.* [20] introduced the following approximate solutions:

$$a_1 = -\frac{\varphi}{2\sqrt{\pi r}} \exp\left[-\frac{1}{4}\left(2\eta - \sqrt{r} + \frac{1}{\sqrt{r}} \right)^2 - \frac{1}{4r} \right],$$

$$b_1 = -\frac{\varphi \sqrt{r}}{2\sqrt{\pi}} \exp\left[-\frac{1}{4}\left(2r\eta - \sqrt{r} + \frac{1}{\sqrt{r}} \right)^2 - \frac{r}{4} \right].$$

An improvement to these approximations were then made by Malyutin *et al.* [23] based on the Feynman-Kac formula [28] which are given by

$$a_1 = -a_0 b_0 + \frac{\sqrt{r}\varphi}{6\sqrt{\pi}} e^{-\eta^2} \left[\operatorname{erf}\left(r\eta + \frac{\sqrt{r}}{2} \right) - \operatorname{erf}\left(r\eta - \frac{\sqrt{r}}{2} \right) \right],$$

$$b_1 = -a_0 b_0 + \frac{e^{-r^2\eta^2}\varphi}{6\sqrt{\pi r}} \left[\operatorname{erf}\left(\eta + \frac{1}{2\sqrt{r}} \right) - \operatorname{erf}\left(\eta - \frac{1}{2\sqrt{r}} \right) \right].$$

At the initial interface $\eta = 0$ these solutions yield

$$\kappa_1 \equiv a_1|_{\eta=0} = -\frac{\varphi}{4} + \frac{\varphi\sqrt{r}}{3\sqrt{\pi}} \operatorname{erf}\left(\frac{\sqrt{r}}{2} \right),$$

$$\kappa_3 \equiv b_1|_{\eta=0} = -\frac{\varphi}{4} + \frac{\varphi}{3\sqrt{\pi r}} \operatorname{erf}\left(\frac{1}{2\sqrt{r}} \right),$$

where κ_1 and κ_3 have been introduced for comparative purposes.

However, the solution to system (8) can be analytically expressed as an integral solution, namely,

$$\frac{a_1}{1 + 2\eta^2} = \chi_1 + S(\eta)\left(\frac{\chi_2}{4} + \int_0^\eta a_0 b_0 P(z) dz \right) - \int_0^\eta a_0 b_0 [\sqrt{\pi} P(z) \operatorname{erf}(z) + 2z] dz, \quad (19a)$$

$$\frac{b_1}{1 + 2r^2\eta^2} = \chi_3 + rS(r\eta)\left(\frac{\chi_4}{4r^2} + \int_0^\eta a_0 b_0 P(rz) dz \right) - r\int_0^\eta a_0 b_0 [\sqrt{\pi} P(rz) \operatorname{erf}(rz) + 2rz] dz, \quad (19b)$$

$$\frac{c_1}{1 + 2s^2\eta^2} = \chi_5 + sS(s\eta)\left(\frac{\chi_6}{4s^2} - \int_0^\eta a_0 b_0 P(sz) dz \right) + s\int_0^\eta a_0 b_0 [\sqrt{\pi} P(sz) \operatorname{erf}(sz) + 2sz] dz, \quad (19c)$$

where the functions P and S are given in Appendix B and the details of this derivation are presented for b_1. The six integration constants denote the following initial interfacial quantities:

$$a_1|_{\eta=0} = \chi_1 \quad \text{and} \quad a_{1\eta}|_{\eta=0} = \chi_2,$$

$$b_1|_{\eta=0} = \chi_3 \quad \text{and} \quad b_{1\eta}|_{\eta=0} = \chi_4,$$

$$c_1|_{\eta=0} = \chi_5 \quad \text{and} \quad c_{1\eta}|_{\eta=0} = \chi_6.$$

Applying the first-order far field conditions, namely,

$$a_1, b_1, c_1 \to 0 \quad \text{as} \quad \eta \to \pm\infty$$

to the solutions in Eq. (19) results in these six conditions,

$$\frac{\sqrt{\pi}\chi_2}{4} - \chi_1 = \int_{-\infty}^0 a_0 b_0 [2z + \sqrt{\pi} P(z) \operatorname{erfc}(-z)] dz,$$

$$\frac{\sqrt{\pi}\chi_2}{4} + \chi_1 = \int_0^\infty a_0 b_0 [2z - \sqrt{\pi} P(z) \operatorname{erfc}(z)] dz,$$

$$\frac{\sqrt{\pi}\chi_4}{4r} - \chi_3 = r\int_{-\infty}^0 a_0 b_0 [2rz + \sqrt{\pi} P(rz) \operatorname{erfc}(-rz)] dz,$$

$$\frac{\sqrt{\pi}\chi_4}{4r} + \chi_3 = r\int_0^\infty a_0 b_0 [2rz - \sqrt{\pi} P(rz) \operatorname{erfc}(rz)] dz,$$

$$\frac{\sqrt{\pi}\chi_6}{4s} - \chi_5 = -s\int_{-\infty}^0 a_0 b_0 [2sz + \sqrt{\pi} P(sz) \operatorname{erfc}(-sz)] dz,$$

$$\frac{\sqrt{\pi}\chi_6}{4s} + \chi_5 = -s\int_0^\infty a_0 b_0 [2sz - \sqrt{\pi} P(sz) \operatorname{erfc}(sz)] dz.$$

These six equations can be evaluated to read as

$$\frac{\sqrt{\pi}\chi_2}{4} - \chi_1 = \frac{\varphi}{8}\left[1 + \frac{4}{r+1} - G(r) - K(1, r, 1) \right],$$

$$\frac{\sqrt{\pi}\chi_2}{4} + \chi_1 = -\frac{\varphi}{8}[3 - G(r) - K(1, r, 1)],$$

$$\frac{\sqrt{\pi}\chi_4}{4r} - \chi_3 = \frac{r\varphi}{8}\left[r + \frac{2}{r} - rG(r) - K(1,r,r)\right],$$

$$\frac{\sqrt{\pi}\chi_4}{4r} + \chi_3 = -\frac{r\varphi}{8}\left[r + \frac{4}{1+r} - rG(r) - K(1,r,r)\right],$$

$$\frac{\sqrt{\pi}\chi_6}{4s} - \chi_5 = -\frac{s\varphi}{8}\left[s + \frac{4}{r+s} - sG(r) - K(1,r,s)\right],$$

$$\frac{\sqrt{\pi}\chi_6}{4s} + \chi_5 = \frac{s\varphi}{8}\left[s + \frac{4}{1+s} - sG(r) - K(1,r,s)\right],$$

where the functions G and K are defined in Appendix A. Solving these six equations yields

$$\chi_1 = \frac{\varphi}{4\pi}\left(\frac{\pi}{r^2-1} - \frac{1}{r} - \frac{(r^2+1)^2}{r^2(r^2-1)}\tan^{-1}(r)\right), \tag{20a}$$

$$\chi_2 = \frac{\varphi(1-r)}{2\sqrt{\pi}(r+1)}, \tag{20b}$$

$$\chi_3 = \frac{\varphi}{4\pi}\left(\frac{\pi(1+r^4)}{2(r^2-1)} - r - \frac{(r^2+1)^2}{r^2-1}\tan^{-1}(r)\right), \tag{20c}$$

$$\chi_4 = \frac{r\varphi(1-r)}{2\sqrt{\pi}(r+1)}, \tag{20d}$$

$$\chi_5 = \frac{s^2\varphi}{2\pi(s^2-r^2)}\left(\frac{\pi}{2} - \frac{r^2-1}{s^2-1}\tan^{-1}(r)\right) + \frac{rs\varphi(r^2+1-2s^2)\tan^{-1}(s^{-1}\sqrt{1+r^2-s^2})}{2\pi(s^2-r^2)(s^2-1)\sqrt{1+r^2-s^2}}, \tag{20e}$$

$$\chi_6 = \frac{s^2\varphi(r-1)}{\sqrt{\pi}(r+s)(s+1)}. \tag{20f}$$

Some of these expressions initially appear to be singular in the following five limits: $r\to 0$, $r\to 1$, $s\to 1$, $s\to\sqrt{1+r^2}$, and $s\to r$; however, by expanding around each limit reveals no such singularities, as expected, since the corrections to the concentrations must remain finite. We notice that all of the χ_i's are proportional to φ.

The quantities χ_1, χ_2, χ_3, and χ_4 further depend on r. The interfacial value of a_1, χ_1, is a monotonic increasing function of r while the interfacial value of b_1, χ_3, is a monotonic decreasing function of r, as illustrated in Fig. 3. Both χ_1 and χ_3 lie between $-\frac{\varphi}{4}$ and $-\frac{\varphi}{8}$ and equal to $-\frac{\varphi}{2\pi}$ at $r=1$.

In Fig. 3 the values κ_1 and κ_3 are also presented. One notices that although κ_1 is close to χ_1 for $r\ll 1$ and $r\simeq 1$, for large r, $\kappa_1\to\infty$ like $\sqrt{r}$. Similarly κ_3 is close to χ_3 for $r\gg 1$ and $r\simeq 1$, but for small r, $\kappa_3\to\infty$ like $1/\sqrt{r}$. Thus as $|r-1|$ increases, one of the solutions in [23] will rapidly diverge from the analytical solution.

The interfacial derivative of a_1, χ_2, is a monotonic decreasing function of r lying between $-\frac{\varphi}{2\sqrt{\pi}}$ and $\frac{\varphi}{2\sqrt{\pi}}$ and taking the value 0 at $r=1$. The interfacial derivative of b_1, χ_4, equals

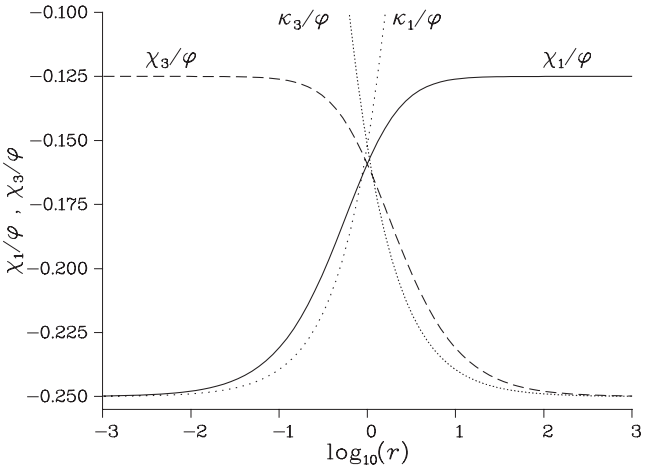

FIG. 3. Analytical solutions of the normalized interfacial values of a_1, χ_1/φ and b_1, χ_3/φ against $\log_{10}(r)$. The approximate solutions κ_1/φ and κ_3/φ are also plotted against $\log_{10}(r)$.

that of a_1 multiplied by r, i.e., $\chi_4=r\chi_2$. Thus χ_4 is zero at $r=0$ and $r=1$ with its maximum value at $r=\sqrt{2}-1$. Hence, the interfacial gradients of a_1 and b_1 are positive for $r<1$ and negative for $r>1$ and further the interfacial gradient of $b_1\to-\infty$ as $r\to\infty$. Physically letting r tend to infinity with D_a fixed is equivalent to letting D_b tend to zero, which will result in a large gradient at $\eta=0$; thus it is consistent to expect χ_4 to tend to infinity in this limit.

As product C can diffuse at a different rate to each of the reactants it depends on the three parameters: φ, r, and s. The interfacial value of c_1, χ_5, is a monotonic decreasing functions of r, but a monotonic increasing function of s lying between 0 and $\frac{\varphi}{4}$. As $r\to 0$ or as $s\to\infty$ then $\chi_5\to\frac{\varphi}{4}$, physically these limits correspond to $D_b\to\infty$ or $D_c\to 0$, respectively. In the limit $s\to\sqrt{1+r^2}$ one obtains

$$\chi_5 = \frac{\varphi(1+r^2)}{2\pi}\left(\frac{\pi}{2} - \frac{1}{r} - \frac{r^2-1}{r^2}\tan^{-1}(r)\right),$$

which takes the value $\frac{\varphi}{4}$ in both the large and small limits of r and has a local minimum at $r=1$ with χ_5 reaching $\varphi(\frac{1}{2}-\frac{1}{\pi})$. Also in the limit $r\to\infty$, $\chi_5\to\frac{\varphi s}{4(s+1)}$. [It is important to note that $\tan^{-1}(iz)\equiv i\tanh^{-1}(z)$, where $i=\sqrt{-1}$ so that χ_5 is always real even when $s^2>1+r^2$.] The interfacial derivative of c_1, χ_6, is a monotonic increasing function of r, but a monotonic decreasing function of s which is zero at $r=1$. If χ_6 is considered as a function of s then it lies between 0 and $\varphi(r-1)/\sqrt{\pi}$.

In the special case when $s=1$, so that species C diffuses at the same rate as reactant A, then $\chi_5=-\chi_1$ and $\chi_6=-\chi_2$ and further Eq. (19) implies that $c_1=-a_1$ which is expected in this case. Similarly, when $s=r$, so that species C diffuses at the same rate as reactant B, then $\chi_5=-\chi_3$ and $\chi_6=-\chi_4$ and now Eq. (19) implies that $c_1=-b_1$.

A. More explicit form of the solution

Although, the forms of the analytical solutions in Eq. (19) with Eq. (20) are convenient due to their concise forms, they

involve pairs of integrals that individually tend to infinity as $|\eta| \to \infty$. This divergence can hinder the accuracy of a numerical evaluation. Using integration by parts the divergent contributions can be removed leading to these more explicit forms of the solutions,

$$a_1 = (1+2\eta^2)\left(\chi_1 + \zeta_A + \frac{\varphi(r^2+1)}{8(1-r^2)} - \frac{\varphi(r^2+1)^2 a_0}{4r^2(1-r^2)}\right) + a_0 b_0\left[2\eta^2 + (1+2\eta^2)\left(\frac{1}{2r^2} + \frac{1}{1-r^2} - \eta^2\right)\right] - \eta a_0 b_{0\eta}\left(\frac{1}{2r^2} + \frac{1}{1-r^2} + \frac{\eta^2}{r^2}\right) - \frac{\varphi\eta(r^2+1)^2 a_{0\eta}}{4r^2(1-r^2)} + \eta b_0 a_{0\eta}\left(\frac{1}{2r^2} + \frac{1}{1-r^2} - \eta^2\right) - \frac{\eta^2}{2r^2} a_{0\eta} b_{0\eta}, \quad (21a)$$

$$b_1 = (1+2r^2\eta^2)\left(\chi_3 + \zeta_B + \frac{\varphi(r^2+1)}{8(r^2-1)} - \frac{(r^2+1)^2 b_0}{4(r^2-1)}\right) + r^2 a_0 b_0\left[2\eta^2 + (1+2r^2\eta^2)\left(\frac{1}{2} + \frac{1}{r^2-1} - \eta^2\right)\right] - r^2\eta b_0 a_{0\eta}\left(\frac{1}{2} + \frac{1}{r^2-1} + r^2\eta^2\right) - \frac{(r^2+1)^2\eta b_{0\eta}}{4(r^2-1)} + r^2\eta a_0 b_{0\eta}\left(\frac{1}{2} + \frac{1}{r^2-1} - \eta^2\right) - \frac{r^2\eta^2}{2} a_{0\eta} b_{0\eta}, \quad (21b)$$

$$c_1 = (1+2s^2\eta^2)\left(\chi_5 + \zeta_C + \frac{\varphi s^2(1-r^2)\mathrm{erf}(s\eta)}{4(s^2-r^2)(s^2-1)}\right) + s^2\eta\left[\frac{a_0 b_{0\eta}}{s^2-r^2} + \frac{b_0 a_{0\eta}}{s^2-1} + \frac{s\varphi(1-r^2)e^{-s^2\eta^2}}{2\sqrt{\pi}(s^2-r^2)(s^2-1)}\right] + \frac{\varphi r s^2\eta(2s^2-r^2-1)}{2\sqrt{\pi}(s^2-r^2)(s^2-1)} \frac{\mathrm{erf}(\sqrt{r^2+1-s^2}\,\eta)}{\sqrt{r^2+1-s^2}} e^{-s^2\eta^2} - 2s^2\eta^2 a_0 b_0, \quad (21c)$$

where the functionals ζ_A, ζ_B, and ζ_C are given by

$$\zeta_A = 2\int_0^\eta a_0\left(z b_0 - \frac{b_{0z}}{1-r^2}\right)dz, \quad (22a)$$

$$\zeta_B = 2r^2\int_0^\eta b_0\left(z a_0 - \frac{a_{0z}}{r^2-1}\right)dz, \quad (22b)$$

$$\zeta_C = \frac{\varphi r s^2(2s^2-r^2-1)}{2(s^2-r^2)(s^2-1)}\int_0^\eta \frac{\mathrm{erf}(\sqrt{r^2+1-s^2}\,z)}{\sqrt{\pi}\sqrt{r^2+1-s^2}} e^{-s^2z^2} dz + s^2\int_0^\eta \frac{a_0 b_{0z}}{s^2-r^2} + \frac{b_0 a_{0z}}{s^2-1} dz. \quad (22c)$$

The expressions in (21) were verified as solutions of system (8) using the symbolic software MAPLE 8 [29]. In general one must use numerical integration to evaluate ζ_A, ζ_B, and ζ_C and hence obtain the solutions a_1, b_1, and c_1.

As expected, a_1 and b_1 are found to be nonpositive while c_1 is non-negative. Further one finds that a_1 and b_1 are always greater than $-\varphi/2$. This introduces an additional restraint on the validity of the small-time asymptotic expansion that $t < \varphi^{-1}$ when $\varphi > 1$ or $t < 1$ when $\varphi < 1$, so that the concentrations a and b remain non-negative. In dimensional quantities these constraints become $kT < \min(1/\hat{A}_0, 1/\hat{B}_0)$.

B. Immobile reactant limit

As ζ_A/φ and ζ_B/φ defined in Eq. (22) only depend on the parameter r, their asymptotic limits as $r \to 0$ or $r \to \infty$ can be determined. Without loss of generality only the limits as $r \to 0$ need to be considered and are determined in Appendix C. Thus one can obtain the two outer solutions of a_1 and b_1. For $\eta \gg 1$, using $a_0 = 0$, we have

$$a_{1+}^{out} = 0, \quad (23a)$$

$$b_{1+}^{out} = (1+2r^2\eta^2)\frac{b_0 - \varphi}{4} + \frac{\eta}{4} b_{0\eta} \quad (23b)$$

and for $\eta \ll -1$, using $a_0 = 1$, the solutions are

$$a_{1-}^{out} = -(1+2r^2\eta^2)b_0 - \eta b_{0\eta}, \quad (23c)$$

$$b_{1-}^{out} = (6r^2\eta^2 - 1)\frac{b_0}{4} + \frac{3\eta}{4} b_{0\eta}, \quad (23d)$$

which are valid for $r \ll 1$ with $|\eta| \gg 1$. In general a similar asymptotic solution for c_1 has not been found; however, in the special cases $s = 1$ or $s = r$ we recall that one obtains $c_1 = -a_1$ or $c_1 = -b_1$, respectively.

We notice that a_{1-}^{out} and b_{1-}^{out} satisfy Eq. (8) using $a_0 = 1$ while a_{1+}^{out} and b_{1+}^{out} satisfy Eq. (8) using $a_0 = 0$. Although these solutions are not valid near $\eta = 0$ we notice that the outer solutions for b_1 and its first derivative are continuous at $\eta = 0$ with $b_1 = -\varphi/8$ and $b_{1\eta} = r\varphi/\sqrt{4\pi}$ which agree with the analytical values of χ_3 and χ_4, respectively, in the limit as $r \to 0$. One finds that b_{1-}^{out} has a local minimum located at $\eta = -\lambda/r$, where $\lambda \approx 0.2423$ which has been determined from the root of the equation $3\sqrt{\pi}\lambda\,\mathrm{erfc}(\lambda) = e^{-\lambda^2}$. In dimensional quantities the position of the local minimum in b_1 is at

$$X = -2\lambda\sqrt{D_b T} \quad (24)$$

in this limit. The minimum value of b_{1-}^{out} is thus given by $-\frac{1}{8}(1+12\lambda^2)\mathrm{erfc}(\lambda) \approx -0.1559$. Now using Eq. (16), as $r \to 0$, we find that the predicted position of the first moment of the reaction rate, $x_f/\sqrt{4t} = -\sqrt{\pi}/(4r) \approx -0.4431/r$, is nearly twice as far to the left of $\eta = 0$ as the position of the minimum of b_1, although they both scale with r^{-1}.

At $\eta = 0$, the outer solutions for a_1 are discontinuous with $a_{1+}^{out} = 0$ while $a_{1-}^{out} = -\varphi/2$. The solution $a_{1+}^{out} = 0$ is to be expected in this limit since $r \to 0$ means that reactant A diffuses much slower than reactant B so that very little of reactant A is present in $\eta > 0$. The inner solutions for a_1 and b_1, between the two outer solutions, are obtained in an inner region, $|r\eta| \ll 1$, by expanding b_0 in a Taylor series to yield

$$a_1^{in} = -\frac{\varphi}{2}\left[a_0 + \frac{4r}{3\sqrt{\pi}}(3\eta a_0 + a_{0\eta})\right] - \frac{\varphi r^2}{2}[(1+2\eta^2)a_0 + \eta a_{0\eta}], \tag{25a}$$

$$b_1^{in} = \frac{\varphi}{2}\left[-\frac{1}{4} + \frac{r\eta}{\sqrt{\pi}}\right] + \frac{\varphi r^2}{2}\left(\eta a_{0\eta} + (1+2\eta^2)a_0 - \frac{3+2\eta^2}{4}\right), \tag{25b}$$

with terms of order r^3 and higher neglected. We find that a_1^{in} has a local minimum located at $\eta = -\sqrt{\ln(\frac{1}{4r})}$. In dimensional quantities the position of the local minimum in a_1 is at

$$X = -\sqrt{2D_a T}\sqrt{\ln\left(\frac{D_b}{4D_a}\right)} \tag{26}$$

in this limit. The position of the minimum of a_1 as $r \to 0$ is not quite as far to the left as the predicted position of the maximum reaction rate, $x_m/\sqrt{4t}$, given by Eq. (11), although they both involve the square root of the logarithm of r^{-1}.

In summary, in the limit $r \to 0$ we find that the local minimum in b_1 is located around the same order of magnitude as the first moment of the reaction rate, while the local minimum in a_1 is located around the same order of magnitude as the position of the maximum reaction rate.

The asymptotic solutions as $r \to \infty$ can be obtained from the solutions in the limit as $r \to 0$ by reversing the dimensional roles of A and B. In particular, the outer solutions for $r\eta \gg 1$, using $b_0 = \varphi$, are given by

$$a_{1+}^{out} = \frac{\varphi}{4}(6\eta^2 - 1)a_0 + \frac{3\varphi}{4}\eta a_{0\eta}, \tag{27a}$$

$$b_{1+}^{out} = -\varphi(1+2\eta^2)a_0 - \varphi\eta a_{0\eta} \tag{27b}$$

and for $r\eta \ll -1$, using $b_0 = 0$, the solutions are

$$a_{1-}^{out} = \varphi(1+2\eta^2)\frac{a_0 - 1}{4} + \frac{\varphi\eta}{4}a_{0\eta}, \tag{27c}$$

$$b_{1-}^{out} = 0, \tag{27d}$$

which are valid for $r \gg 1$ and $|r\eta| \gg 1$. Now the outer solutions for a_1 and its first derivative are continuous at $\eta = 0$ with $a_1 = -\varphi/8$ and $a_{1\eta} = -\varphi/\sqrt{4\pi}$ which agree with the analytical values of χ_1 and χ_2, respectively, in the limit as $r \to \infty$. Further, a_{1+}^{out} has a local minimum located at $\eta = \lambda$. Then using Eq. (16), as $r \to \infty$, we find that the predicted position of the first moment of the reaction rate, $x_f/\sqrt{4t} = \sqrt{\pi}/4 \approx 0.4431$ is nearly twice as far to the right of $\eta = 0$ as the position of the minimum of a_1. Similarly the inner solution can be obtained for $|\eta| \ll 1$ in the limit as $r \to \infty$ by expanding a_0 in a Taylor series.

In Fig. 4 profiles of a_1/φ and b_1/φ are illustrated for values of r tending to zero. The asymptotic outer solution (23) as $r \to 0$ is illustrated by the solid line. The profiles of a_1 and b_1 get wider and wider as $r \to 0$ and so the profiles are plotted against $r\eta$. As $r \to 0$ the curves approach the asymptotic small r limit. For $r < 1$, both a_1 and b_1 have local minima in $\eta < 0$. As $r \to 0$ the minimum of a_1 approaches $-\frac{\varphi}{2}$. Further, a_1 decays much more rapidly in $\eta > 0$ than in $\eta < 0$ so that, as predicted, a_1 has a very sharp minimum in the small r limit.

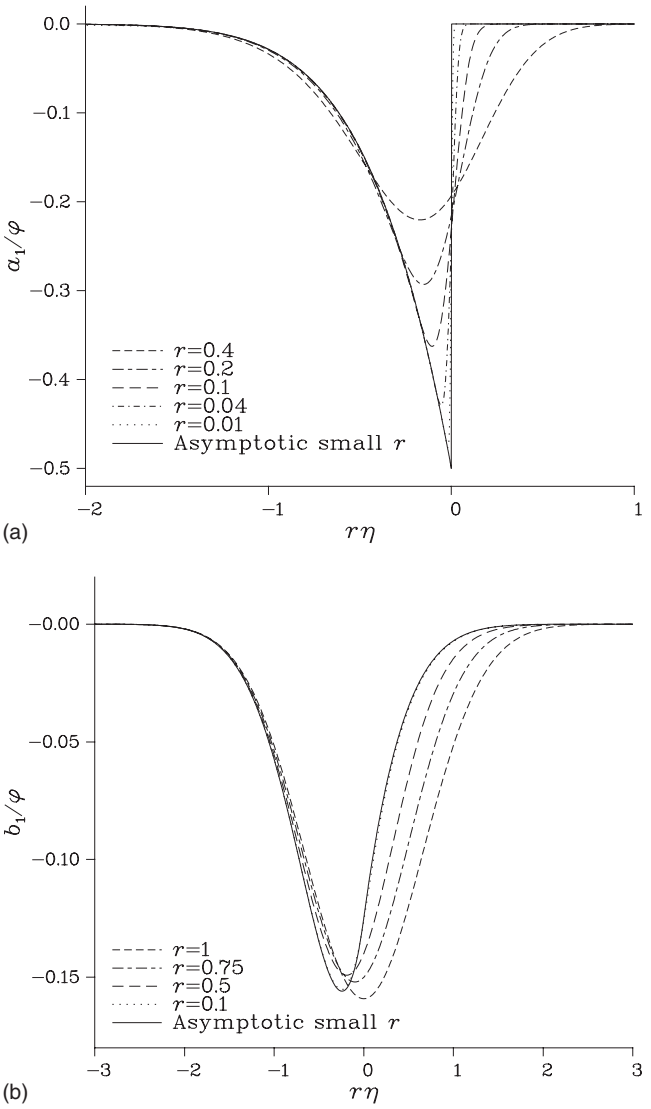

FIG. 4. Profiles of the normalized first-order solutions (a) a_1/φ and (b) b_1/φ against $r\eta$ as $r \to 0$. The solid line denotes the asymptotic outer solution for small r given by Eq. (23).

In Fig. 5 profiles of a_1/φ and b_1/φ are illustrated for values of r tending to infinity. The asymptotic outer solution [Eq. (27)], as $r \to \infty$, is illustrated by the solid line. In this limit their widths become independent of r. As $r \to \infty$ the curves approach the asymptotic large r limit. For $r > 1$, both a_1 and b_1 have local minima in $\eta > 0$. As $r \to \infty$ the minimum of b_1 approaches $-\frac{\varphi}{2}$. Further, b_1 decays much more rapidly in $\eta < 0$ than in $\eta > 0$ so that b_1 has a very sharp minimum in the large r limit.

Hence, the outer solutions which are much simpler than the full solutions have been shown to reveal the dominant behavior of the functions a_1 and b_1 in the limit $r \to 0$ and $r \to \infty$. In Sec. VII the integral properties of the full solutions will be addressed for any value of r.

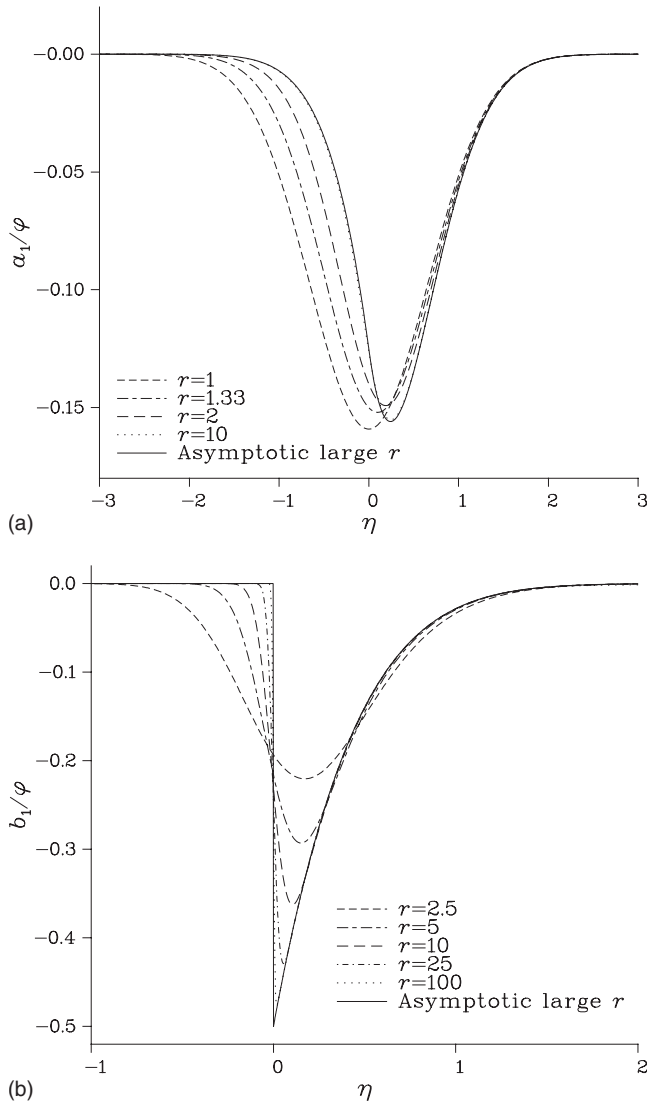

FIG. 5. Profiles of the normalized first-order solutions: (a) a_1/φ and (b) b_1/φ against η as $r\to\infty$. The solid line denotes the asymptotic outer solution for large r given by Eq. (27).

VII. FIRST-ORDER MOMENTS

In this section the properties of the first-order solutions are examined through their moments.

A. Zeroth moment

First the zeroth moment of each equation in Eq. (8) is considered. Integrating each equation over the positive and negative ranges using integration by parts and using the analytical solutions at $\eta=0$, we obtain the following six conditions:

$$\int_{-\infty}^{0} a_1 d\eta - \frac{\chi_2}{6} = \int_{-\infty}^{0} b_1 d\eta - \frac{\chi_4}{6r^2} = -\int_{-\infty}^{0} c_1 d\eta + \frac{\chi_6}{6s^2} = -\varphi\frac{1+F(1/r)}{6\sqrt{\pi r}},$$

$$\int_{0}^{\infty} a_1 d\eta + \frac{\chi_2}{6} = \int_{0}^{\infty} b_1 d\eta + \frac{\chi_4}{6r^2} = -\int_{0}^{\infty} c_1 d\eta - \frac{\chi_6}{6s^2} = -\varphi\frac{1+F(r)}{6\sqrt{\pi}},$$

where the function F is defined in Appendix A. We notice that pairing up the equations yields the following conservation of mass relationships, namely,

$$\int_{-\infty}^{\infty} a_1 d\eta = \int_{-\infty}^{\infty} b_1 d\eta = -\int_{-\infty}^{\infty} c_1 d\eta = -\frac{2}{3} I_0. \tag{28}$$

This is qualitatively expected. The quantities a_1 and b_1 are the amount of A and B consumed by the reaction while c_1 is the amount of C produced from the reaction. As A and B are consumed at the same rate thus the total amounts of a_1 and b_1 are equal. Further, as C is produced at the same rate at which A and B are consumed, the total amount of c_1 should equal the total amount of $-a_1$. Returning to species C in the x and t coordinates allows one to write

$$\int_{-\infty}^{\infty} c dx \simeq 2t^{3/2}\int_{-\infty}^{\infty} c_1 d\eta = \frac{4I_0}{3} t^{3/2}. \tag{29}$$

Hence, to first order, the small-time asymptotic total amount of C present scales with $t^{3/2}$ which is to be expected since $\frac{d}{dt}\int_{-\infty}^{\infty} c dx = \int_{-\infty}^{\infty} R dx$, which agrees with the result following Eq. (14). On physical grounds this scaling makes sense as the maximum concentration of C scales with t and the width of the distribution of C scales with $\sqrt{t}$ so that the total amount of C scales with the product of these scalings, namely, $t^{3/2}$.

B. First moment

Second, each equation in Eq. (8) is integrated over the positive and negative ranges, with the weight function η, using integration by parts and using the analytical solutions at $\eta=0$, we obtain the following six conditions:

$$\int_{-\infty}^{0} \eta a_1 d\eta + \frac{\chi_1}{8} = \int_{-\infty}^{0} \eta b_1 d\eta + \frac{\chi_3}{8r^2} = -\int_{-\infty}^{0} \eta c_1 d\eta - \frac{\chi_5}{8s^2} = \frac{\varphi}{32r^2}[1+G(1/r)],$$

$$\int_{0}^{\infty} \eta a_1 d\eta - \frac{\chi_1}{8} = \int_{0}^{\infty} \eta b_1 d\eta - \frac{\chi_3}{8r^2} = -\int_{0}^{\infty} \eta c_1 d\eta + \frac{\chi_5}{8s^2} = -\frac{\varphi}{32}[1+G(r)].$$

We notice that pairing up the equations yields the following relationships:

$$\int_{-\infty}^{\infty} \eta a_1 d\eta = \int_{-\infty}^{\infty} \eta b_1 d\eta = -\int_{-\infty}^{\infty} \eta c_1 d\eta = -\frac{1}{2} I_1. \tag{30}$$

Using Eqs. (28) and (30) allows the small-time asymptotic center of mass of the product to be obtained,

$$x_c = \frac{\int_{-\infty}^{\infty} x c_1 dx}{\int_{-\infty}^{\infty} c_1 dx} = 2\sqrt{t}\frac{\int_{-\infty}^{\infty} \eta c_1 d\eta}{\int_{-\infty}^{\infty} c_1 d\eta} = \frac{3I_1}{2I_0}\sqrt{t} = \frac{3}{4}x_f, \quad (31)$$

which shows that the center of mass of the product initially lags behind the center of mass of the reaction rate. One notes that the large time asymptotic center of mass of the product can also be expressed in terms of the large time asymptotic center of mass of the reaction rate as $x_c = \frac{1}{2}x_f$, found in [17]. Further, Eqs. (28) and (30) reveal that a_1, b_1, and c_1 all have identical first moments so that their centers of mass are all at the same place, x_c.

C. Second moment

Third, each equation in Eq. (8) is integrated over the positive and negative ranges, with the weight function η^2; using integration by parts one obtains the following six equations:

$$\begin{aligned} -\varphi\frac{1+H(1/r)}{30\sqrt{\pi}r^3} &= \int_{-\infty}^{0} \eta^2 a_1 d\eta + \varphi\frac{1+F(1/r)}{30\sqrt{\pi r}} - \frac{\chi_2}{30} \\ &= \int_{-\infty}^{0} \eta^2 b_1 d\eta + \varphi\frac{1+F(1/r)}{30\sqrt{\pi}r^{5/2}} - \frac{\chi_4}{30r^4} \\ &= -\int_{-\infty}^{0} \eta^2 c_1 d\eta + \varphi\frac{1+F(1/r)}{30\sqrt{\pi r}s^2} + \frac{\chi_6}{30s^4}, \end{aligned}$$

$$\begin{aligned} -\varphi\frac{1+H(r)}{30\sqrt{\pi}} &= \int_{0}^{\infty} \eta^2 a_1 d\eta + \varphi\frac{1+F(r)}{30\sqrt{\pi}} + \frac{\chi_2}{30} \\ &= \int_{-\infty}^{0} \eta^2 b_1 d\eta + \varphi\frac{1+F(r)}{30\sqrt{\pi}r^2} + \frac{\chi_4}{30r^4} \\ &= -\int_{-\infty}^{0} \eta^2 c_1 d\eta + \varphi\frac{1+F(r)}{30\sqrt{\pi}s^2} - \frac{\chi_6}{30s^4}, \end{aligned}$$

where the function H is defined in Appendix A. We notice that pairing up the equations yields the following relationships:

$$\int_{-\infty}^{\infty} \eta^2 a_1 d\eta = -\tfrac{2}{5}I_2 - \tfrac{2}{15}I_0, \quad (32a)$$

$$\int_{-\infty}^{\infty} \eta^2 b_1 d\eta = -\frac{2}{5}I_2 - \frac{2}{15r^2}I_0, \quad (32b)$$

$$\int_{-\infty}^{\infty} \eta^2 c_1 d\eta = \frac{2}{5}I_2 + \frac{2}{15s^2}I_0. \quad (32c)$$

The width of the product can be measured using the second moment of c_1 and is written as

$$\begin{aligned} w_c^2 &= \frac{\int_{-\infty}^{\infty} (x-x_c)^2 c_1 dx}{\int_{-\infty}^{\infty} c_1 dx} = 4t\frac{\int_{-\infty}^{\infty} \eta^2 c_1 d\eta}{\int_{-\infty}^{\infty} c_1 d\eta} - x_c^2 \\ &= \frac{128(2r^4+r^2+2) - 45\pi(r^2-1)^2}{320r^2(r^2+1)}t + \frac{4t}{5s^2} \end{aligned} \quad (33)$$

so that w_c scales like $\sqrt{t}$. Similarly the widths of a_1 and b_1 are given by their second moments to yield

$$w_a^2 = \frac{128(4r^4+3r^2+2) - 45\pi(r^2-1)^2}{320r^2(1+r^2)}t, \quad (34a)$$

$$w_b^2 = \frac{128(2r^4+3r^2+4) - 45\pi(r^2-1)^2}{320r^2(1+r^2)}t, \quad (34b)$$

which both monotonically decrease as r increases, with w_a and w_b scaling with $\sqrt{t}$. The limits in Eq. (34) reveal that as $r \to 0$, the square of the widths approaches the limits

$$w_a^2 \to \frac{256-45\pi}{320r^2}t \quad \text{and} \quad w_b^2 \to \frac{512-45\pi}{320r^2}t.$$

This result could have been obtained directly from the outer solutions (23) obtained in Sec. VI and shows that the widths of a_1 and b_1 tend to infinity like r^{-1} in this limit. As $r \to \infty$, the square of the widths approaches the limits

$$w_a^2 \to \frac{512-45\pi}{320}t \quad \text{and} \quad w_b^2 \to \frac{256-45\pi}{320}t,$$

which only depend on time and so the width becomes independent of r as $r \to \infty$. In dimensional quantities one obtains

$$\frac{W_a^2}{T} = M + \frac{4D_a}{5}, \quad \frac{W_b^2}{T} = M + \frac{4D_b}{5}, \quad \frac{W_c^2}{T} = M + \frac{4D_c}{5},$$

where

$$M = \frac{128(2D_a^2 + D_aD_b + 2D_b^2) - 45\pi(D_a - D_b)^2}{320(D_a + D_b)},$$

which shows that the distribution of each species has a different width and even when the product does not diffuse, its width is given by $\sqrt{MT}$. One notes that in the case when one of the reactants does not diffuse, say reactant B, then $W_a \approx 1.8W_b$, so that the width of the reactant that diffuses is only approximately 1.8 times the width of the nondiffusing reactant. Further all of the widths tend to infinity when either D_a or D_b tends to infinity and further $W_c \to \infty$ as $D_c \to \infty$. As expected the diffusion coefficient of the product only affects its width and not its center of mass or production rate.

Although in practice the two reactants and the product will diffuse at different rates, in many studies, for simplicity, they are taken as equal, hence in Appendix D the moments of this special case when $r=s=1$ are also presented.

All the quantities obtained in this study have been found to be in excellent agreement with the corresponding numerically obtained quantities for small times, however, the length of time that the solutions are valid does depend on the parameter values used.

VIII. CONCLUSIONS

In conclusion, various analytical properties of the reaction front generated by an $A+B\rightarrow C$ reaction have been obtained in the small-time asymptotic limit. The corrections to the zeroth-order solutions are expressed analytically using single integrals with the concentration and their gradients at the initial interface obtained exactly. The first moment of the reaction front is found to travel faster than the position of the maximum reaction rate in the small-time asymptotic limit. First-order solutions in time for the reactant concentrations are obtained in the limit when one reactant diffuses much faster than the other one. Here one finds that the position where the reaction rate is maximum is on the length scale of the slowest diffusing reactant while the first moment of the reaction rate and the width of the reaction front are on the length scale of the fastest diffusing reactant. If the sum of the initial reactant concentrations is fixed, then the fastest reaction rate is obtained when equal concentrations are used.

Analytical concentration profiles are expressed using a single integral solution which is numerically much easier to deal with than the previous double integral solutions existing in the literature. At small times the length scale is very small so that a numerical solution to the full system of reaction-diffusion equations can lead to inaccurate results. This study provides a benchmark to test numerical codes in the small-time asymptotic limit.

The first-order solutions are found to remain finite for all parameter values unlike the approximations presented in the literature which have serious problems when the ratio of the diffusion coefficients of the reactants is not close to unity. The study also provides an asymptotic solution for the case when the ratio of the reactant diffusion coefficients is large. If one of the reactants diffuses much faster than the other, then the slowest diffusing reactant has a much sharper gradient in its first correction to the solutions near the reaction front than the faster diffusing reactant. This study provides quantitative measures of the solutions analytically. Finally, the center of mass of the product is found to be initially located at three quarters of the position of the center of mass of the reaction rate.

ACKNOWLEDGMENTS

P.M.J.T. would like to thank Anne De Wit for constant support as well as Manoranjan Mishra and Damian Strier for fruitful discussions. The author acknowledges Prodex (Belgium) for financial support.

APPENDIX A: USEFUL INTEGRALS

The following definite integral results have been utilized for $\alpha>0$:

$$\int_0^\infty \operatorname{erfc}(\alpha z)\operatorname{erfc}(\beta z)dz = \frac{1-F(\beta/\alpha)}{\sqrt{\pi}\alpha},$$

$$\int_0^\infty z\,\operatorname{erfc}(\alpha z)\operatorname{erfc}(\beta z)dz = \frac{1-G(\beta/\alpha)}{4\alpha^2},$$

$$\int_0^\infty z^2\,\operatorname{erfc}(\alpha z)\operatorname{erfc}(\beta z)dz = \frac{1-H(\beta/\alpha)}{3\sqrt{\pi}\alpha^3},$$

$$\int_0^\infty \operatorname{erfc}(\alpha z)\operatorname{erfc}(\beta z)P(\beta z)dz = \frac{2\alpha^2+\alpha\beta+\beta^2}{2\sqrt{\pi}\alpha^2(\alpha+\beta)},$$

$$\int_0^\infty \operatorname{erfc}(\alpha z)\operatorname{erfc}(\beta z)\operatorname{erfc}(\gamma z)P(\gamma z)dz = \frac{K(\alpha,\beta,\gamma)}{2\sqrt{\pi}},$$

where the fourth and fifth integrals are valid under the additional constraints $\beta>-\alpha$ and $\gamma>-\sqrt{\alpha^2+1/2|\beta|(|\beta|+\beta)}$, respectively, where the function P is given by Eq. (B2) in Appendix B and the remaining functions are

$$F(z) = \frac{\sqrt{z^2+1}-1}{z},$$

$$G(z) = \frac{2}{\pi}\left(\frac{1}{z}+\frac{z^2-1}{z^2}\tan^{-1}(z)\right),$$

$$H(z) = \frac{2z^4+z^2+2-2\sqrt{z^2+1}}{2z^3\sqrt{z^2+1}},$$

$$K(\alpha,\beta,\gamma) = \alpha\frac{L\left(\frac{\alpha}{\beta},\frac{\gamma}{\beta}\right)}{\beta^2}+\beta\frac{L\left(\frac{\beta}{\alpha},\frac{\gamma}{\alpha}\right)}{\alpha^2}+\gamma\frac{1-G\left(\frac{\alpha}{\beta}\right)}{\beta^2},$$

$$L(x,y) = \frac{2\pi-\frac{4\tan^{-1}(\sqrt{x^2+1-y^2}/y)}{\sqrt{x^2+1-y^2}}-\frac{4y}{x}\tan^{-1}x}{\pi(x^2-y^2)}.$$

The functions F, G, and H are monotonic increasing functions of z lying between 0 and 1. We note that $\beta[1-F(\beta/\alpha)]\equiv\alpha[1-F(\alpha/\beta)]$, $\beta^2[1-G(\beta/\alpha)]\equiv\alpha^2[1-G(\alpha/\beta)]$, and $\beta^3[1-H(\beta/\alpha)]\equiv\alpha^3[1-H(\alpha/\beta)]$. The function L is a monotonic decreasing function of x and y that lies between 0 and 1. In the special case when $y=x$, the function L reduces to $1-G(x)$. We notice that $K(1,r,1)=[2\pi r-8\tan^{-1}(r)]/\pi(r^2-1)+2[1-G(r)]$ and $K(1,1,1)=3-\frac{6}{\pi}$.

APPENDIX B: AN INTEGRAL SOLUTION

Starting from Eq. (8b), namely,

$$b_1-\frac{\eta}{2}b_{1\eta} = \frac{b_{1\eta\eta}}{4r^2}-a_0b_0,$$

the analytical solution shall be constructed. By substituting $b_1=(1+2r^2\eta^2)U$ into Eq. (8b) yields

$$-\frac{\eta}{2}(1+2r^2\eta^2)U_\eta = 2\eta U_\eta + (1+2r^2\eta^2)\frac{U_{\eta\eta}}{4r^2} - a_0 b_0.$$

Then by substituting $U_\eta = (1+2r^2\eta^2)^{-2}V$ into the above equation yields

$$V_\eta + 2r^2\eta V = 4r^2 a_0 b_0 (1+2r^2\eta^2).$$

Using the integration factor $e^{r^2\eta^2}$ one obtains

$$V = 4r^2 e^{-r^2\eta^2}\left(\frac{\chi_4}{4r^2} + \int_0^\eta a_0 b_0 (1+2r^2y^2)e^{r^2y^2}dy\right),$$

where χ_4 is the integration constant. This means that

$$U_\eta = \frac{4r^2 e^{-r^2\eta^2}}{(1+2r^2\eta^2)^2}\left(\frac{\chi_4}{4r^2} + \int_0^\eta a_0 b_0 (1+2r^2y^2)e^{r^2y^2}dy\right)$$

and hence the general solution to Eq. (8b) can be expressed by the following double integral solution:

$$\frac{b_1}{1+2r^2\eta^2} = \chi_3 + \frac{\chi_4}{4r^2}\int_0^\eta \frac{4r^2 e^{-r^2z^2}}{(1+2r^2z^2)^2}dz + \int_0^\eta \frac{4r^2 e^{-r^2z^2}}{(1+2r^2z^2)^2}\int_0^z a_0 b_0 (1+2r^2y^2)e^{r^2y^2}dydz, \tag{B1}$$

where χ_3 is the integration constant. It is useful to define

$$Q(z) = \frac{4e^{-z^2}}{(1+2z^2)^2}, \quad P(z) = (1+2z^2)e^{z^2}, \tag{B2}$$

so that the solution can be written as

$$\frac{b_1}{1+2r^2\eta^2} = \chi_3 + \frac{\chi_4}{4r^2}\int_0^\eta r^2 Q(rz)dz + \int_0^\eta r^2 Q(rz)\left(\int_0^z a_0 b_0 P(ry)dy\right)dz.$$

Applying integration by parts to the double integral yields

$$\frac{b_1}{1+2r^2\eta^2} = \chi_3 + \int_0^\eta r^2 Q(rz)dz\int_0^\eta a_0 b_0 P(rz)dz + \frac{\chi_4}{4r^2}\int_0^\eta r^2 Q(rz)dz - \int_0^\eta a_0 b_0 P(rz)\int_0^z r^2 Q(ry)dydz.$$

Finally using the result

$$\int_0^\eta rQ(rz)dz = S(r\eta), \quad \text{where } S(z) = \sqrt{\pi}\,\mathrm{erf}(z) + \frac{2z}{P(z)}$$

the general solution to Eq. (8b) can be expressed in terms of two single integrals as

$$\frac{b_1}{1+2r^2\eta^2} = \chi_3 + rS(r\eta)\left(\frac{\chi_4}{4r^2} + \int_0^\eta a_0 b_0 P(rz)dz\right) - \int_0^\eta a_0 b_0 P(rz) rS(rz)dz. \tag{B3}$$

APPENDIX C: ASYMPTOTIC SOLUTIONS

The asymptotic behavior of ζ_A and ζ_B in the limit $r\to 0$ will be considered here. For convenience we write

$$\zeta_A = 2N_1 - \frac{2}{1-r^2}N_2, \quad \zeta_B = 2r^2 N_1 - \frac{2r^2}{r^2-1}N_3, \tag{C1}$$

where

$$N_1 = \int_0^\eta z a_0 b_0 dz, \quad N_2 = \int_0^\eta a_0 b_{0z} dz, \quad N_3 = \int_0^\eta b_0 a_{0z} dz.$$

Using integration by parts $N_3 \equiv a_0 b_0 - \frac{\varphi}{4} - N_2$, so that N_1 and N_2 are the only terms that cannot be represented analytically.

We shall now obtain the asymptotic limits of N_1 and N_2 as $r\to 0$ in an inner region, $|r\eta| \ll 1$, and in an outer region, $|\eta| \gg 1$. In the inner region, both r and $|r\eta|$ are considered as small quantities so that b_0 and $b_{0\eta}$ can be replaced by their Taylor series approximations while the full solution for a_0 is kept. These yield the following inner solutions:

$$N_1^{in} = \frac{\varphi}{16}[1 + (4\eta^2 - 2)a_0 + 2\eta a_{0\eta}] + \frac{\varphi r}{6\pi}(1 + 2\sqrt{\pi}\eta^3 a_0 + \sqrt{\pi}a_{0\eta}) + \mathcal{O}(r^3),$$

$$N_2^{in} = \frac{\varphi r}{2\pi}(1 + 2\sqrt{\pi}\eta a_0 + \sqrt{\pi}\eta a_{0\eta}) - \frac{\varphi r^3}{6\pi}[1 + 2\sqrt{\pi}\eta^3 a_0 + \sqrt{\pi}(1+\eta^2)a_{0\eta}] + \mathcal{O}(r^5),$$

where the superscript *in* is used to denote the inner solutions which are valid when $r \ll 1$ for $|r\eta| \ll 1$.

In the outer region $|\eta|$ is large, but $|r\eta|$ is assumed order unity so that a_0 becomes a constant and the full solutions for b_0 and $b_{0\eta}$ are kept. If $\eta > 0$ then a_0 can be treated as zero so that there are no further cumulative contributions to N_1 and N_2 and the functions tend to the constants,

$$N_{1+}^{out} = \varphi\frac{1+G(r)}{16}, \quad N_{2+}^{out} = \frac{\varphi}{2\pi}\tan^{-1}(r), \tag{C2}$$

where the superscript *out* is used to denote the outer solutions and the subscript + denotes that this is for $\eta > 0$. If $\eta < 0$ then a_0 can be treated as unity as the corrections are exponentially small in η. Thus we can analytically obtain

$$N_{1-}^{out} = \varphi\frac{2 + r^2[G(r)-1]}{16r^2} + \frac{\eta b_{0\eta}}{4r^2} + \frac{2r^2\eta^2 - 1}{4r^2}b_0, \tag{C3a}$$

$$N_{2-}^{out} = b_0 + \frac{\varphi}{2\pi}\tan^{-1}(r) - \frac{\varphi}{2}, \tag{C3b}$$

where the subscript − denotes that this is for $\eta<0$.

APPENDIX D: EQUIVALENT SPECIES

If all three species have the same diffusive rate then this problem can be simplified. By setting $s=r=1$ and defining $u=a+c$ and $v=b+c$, then the quantities u and v satisfy the nonreactive equations. Further, u and v satisfy the far field boundary conditions of a and b, respectively. Thus $u\equiv a_0$ and $v\equiv b_0$. Returning to the concentrations a, b, and c, one can write

$$a = a_0 - c, \quad b = b_0 - c. \tag{D1}$$

Thus, in the small-time expansion, one obtains the identities $a_1=b_1=-c_1$. It is useful to note that the first-order solutions in Eq. (21) can be simplified when $r=s=1$ to

$$\begin{aligned} a_1 = b_1 = -c_1 = {} & a_0 b_0 \left[\frac{1}{2} + 2\eta^2 - 2\eta^4\right] \\ & + b_{0\eta}(1-2\eta^2)\left[\eta\left(a_0 - \frac{1}{2}\right) + \frac{1}{4}a_{0\eta}\right] \\ & + (1+2\eta^2)\left(2\int_0^\eta a_0 b_0 z\,dz - \frac{\varphi}{4\pi} - \frac{\varphi}{8}\right). \end{aligned} \tag{D2}$$

However, this solution still involves an integral.

For convenience in this appendix R is used to denote the dimensionless reaction rate ab. Up to first order, the reaction rate is given by

$$R = ab \simeq (a_0 + ta_1)(b_0 + tb_1) \simeq a_0 b_0 + (a_1 b_0 + a_0 b_1)t,$$

which can be simplified, using Eq. (D2), to yield

$$R \simeq a_0 b_0 - c_1(a_0 + b_0)t \tag{D3}$$

as $r=s=1$. Recalling that Eq. (10) yields $\alpha_m=0$ when $r=1$ means that in this limit the zeroth-order solution predicts that the location of the maximum reaction rate is at $x_m=0$. Using $c_1 \simeq \chi_5 + \chi_6\eta$ near $\eta=0$ we can expand R in small η to yield

$$R \simeq \frac{\varphi}{4} - \frac{\varphi+1}{2\pi}\varphi t + \frac{1-\varphi}{2\pi}\varphi t\,\eta - \frac{\varphi}{\pi}\eta^2 + \mathcal{O}(t\eta^2, \eta^4), \tag{D4}$$

which is an explicit version of Eq. (27) in [19]. With η and t both small and of the same order, one finds that R has a local maximum at

$$x_m = \frac{1-\varphi}{2\sqrt{\pi}}t^{3/2}, \tag{D5}$$

where the time scaling of $t^{3/2}$ was previously determined in Eq. (28) in [19]. In dimensional quantities one obtains

$$X_m = \frac{\hat{A}_0 - \hat{B}_0}{2\sqrt{\pi}}k\sqrt{D}T^{3/2},$$

where $D=D_a=D_b$ since $r=1$, which reveals that the initial speed of the reaction front is proportional to the kinetic constant k.

Returning to Eq. (D1), in the small-time expansion, one can obtain the second set of identities $a_2=b_2=-c_2$. Then by additionally taking $\varphi=1$, corresponding to equal initial concentrations of A and B, so that $a_0+b_0\equiv 1$, the reactive source term in Eq. (D3) reduces to $R\simeq a_0 b_0 - c_1 t$. The resulting system of second-order equations in Eq. (9) is then fully described by the single equation

$$2c_2 - \frac{\eta c_{2\eta}}{2} = \frac{c_{2\eta\eta}}{4} - c_1. \tag{D6}$$

The far field boundary conditions are then

$$c_2 \to 0 \quad \text{as} \quad |\eta| \to -\infty \quad \text{and} \quad c_2 \to 0 \quad \text{as} \quad |\eta| \to \infty.$$

An integral solution for c_2 could also be obtained as before, however, now the integral involves the first-order solution c_1 and so it is difficult to analytically determine the associated integration constants that must satisfy the far field conditions. Thus such a solution will not be presented here, but instead integral measures of the solution for c_2 will be obtained.

Let us define

$$J_\nu = -\int_{-\infty}^{\infty} \eta^\nu c_1 d\eta \tag{D7}$$

again where ν is a non-negative integer. Setting $r=s=\varphi=1$ in Eqs. (28), (30), and (32) allows the evaluation of I_ν and J_ν to yield

$$I_0 = \frac{1}{\sqrt{2\pi}}, \quad I_1 = 0, \quad I_2 = \frac{5}{12\sqrt{2\pi}},$$

$$J_0 = -\frac{2}{3\sqrt{2\pi}}, \quad J_1 = 0, \quad J_2 = -\frac{3}{10\sqrt{2\pi}}.$$

Using these results allows one to obtain

$$\int_{-\infty}^{\infty} R dx \simeq 2\sqrt{t}(I_0 + J_0 t) = \frac{\sqrt{2t}}{\sqrt{\pi}}\left(1 - \frac{2t}{3}\right),$$

$$\int_{-\infty}^{\infty} xR dx \simeq 4t(I_1 + J_1 t) = 0,$$

$$\int_{-\infty}^{\infty} x^2 R dx \simeq 8t^{3/2}(I_2 + J_2 t) = \frac{\sqrt{2}t^{3/2}}{\sqrt{\pi}}\left(\frac{5}{3} - \frac{6t}{5}\right).$$

Hence, to first order, the small-time asymptotic reaction rate scales with $\sqrt{t}$, the reaction front is stationary, and a measure of the reaction front width, w_f, to first order is given by

$$w_f^2 = \frac{\int_{-\infty}^{\infty} x^2 R dx}{\int_{-\infty}^{\infty} R dx} \simeq \frac{5t - \frac{18t^2}{5}}{3 - 2t} \simeq \frac{5}{3}t - \frac{4t^2}{45}.$$

Hence, expanding w_f in small-time yields

$$w_f \simeq \sqrt{\frac{5t}{3}}\left(1 - \frac{2t}{75}\right), \tag{D8}$$

which is found to be in excellent agreement with, a numerically obtained, reaction front width for small times $t \leq 0.1$, not illustrated.

Not only can the reaction front be analyzed but also the product. First, in this special case $\chi_5 = \frac{1}{2\pi}$ and $\chi_6 = 0$ so that $c|_{x=0} \simeq \frac{t}{2\pi}$ with $c_x|_{x=0} \simeq 0$, which means that the maximum concentration of C is at $x=0$ and this value initially increases linearly with time.

Integrating Eq. (D6) over plus and minus infinities with the weight functions 1, η, and η^2, using integration by parts, yields

$$\int_{-\infty}^{\infty} c_2 d\eta = \frac{2}{5}J_0 = -\frac{4}{15\sqrt{2\pi}}, \tag{D9a}$$

$$\int_{-\infty}^{\infty} \eta c_2 d\eta = \frac{1}{3}J_1 = 0, \tag{D9b}$$

$$\int_{-\infty}^{\infty} \eta^2 c_2 d\eta = \frac{2}{35}J_0 + \frac{2}{7}J_2 = -\frac{13}{105\sqrt{2\pi}}. \tag{D9c}$$

Recalling that $c = tc_1 + t^2 c_2$, Eq. (D9) allows the following analytical results to be stated:

$$\int_{-\infty}^{\infty} c dx = 2\sqrt{t}\int_{-\infty}^{\infty} c d\eta \simeq \frac{2\sqrt{2}}{3\sqrt{\pi}}t^{3/2} - \frac{4\sqrt{2}}{15\sqrt{\pi}}t^{5/2},$$

$$\int_{-\infty}^{\infty} x c dx = 4t\int_{-\infty}^{\infty} \eta c d\eta \simeq 0,$$

$$\int_{-\infty}^{\infty} x^2 c dx = 8t^{3/2}\int_{-\infty}^{\infty} \eta^2 c d\eta \simeq \frac{6\sqrt{2}}{5\sqrt{\pi}}t^{5/2} - \frac{52\sqrt{2}}{105\sqrt{\pi}}t^{7/2}.$$

The position of the center of mass of the product concentration distribution is stationary at $x=0$ and a measure of the width of C, w_c, to first order is given by

$$w_c^2 = \frac{\int_{-\infty}^{\infty} x^2 c dx}{\int_{-\infty}^{\infty} c dx} \simeq \frac{9t - \frac{26}{7}t^2}{5 - 2t} \simeq \frac{9}{5}t - \frac{4t^2}{175}.$$

Hence, we can expand w_c in small time to yield

$$w_c \simeq 3\sqrt{\frac{t}{5}}\left(1 - \frac{2t}{315}\right) \tag{D10}$$

so that not only do both w_c and w_f scale with $\sqrt{t}$ but also their magnitudes are of very similar orders and further both have small negative correction terms.

[1] K. Eckert, M. Acker, and Y. Shi, Phys. Fluids **16**, 385 (2004).
[2] D. A. Bratsun, Y. Shi, K. Eckert, and A. De Wit, Europhys. Lett. **69**, 746 (2005).
[3] Y. Shi and K. Eckert, Chem. Eng. Sci. **61**, 5523 (2006).
[4] A. Riaz, M. Hesse, H. A. Tchelepi, and F. M. Orr, Jr., J. Fluid Mech. **548**, 87 (2006).
[5] A. Zalts, C. El Hasi, D. Rubio, A. Urena, and A. D'Onofrio, Phys. Rev. E **77**, 015304(R) (2008).
[6] L. Rongy, P. M. J. Trevelyan, and A. De Wit, Phys. Rev. Lett. **101**, 084503 (2008).
[7] O. Citri, M. L. Kagan, R. Kosloff, and D. Avnir, Langmuir **6**, 559 (1990).
[8] G. Venzl, J. Chem. Phys. **85**, 2006 (1986).
[9] L. Gálfi and Z. Rácz, Phys. Rev. A **38**, 3151 (1988).
[10] Y.-E. L. Koo and R. Kopelman, J. Stat. Phys. **65**, 893 (1991).
[11] A. Yen and R. Kopelman, Phys. Rev. E **56**, 3694 (1997).
[12] Z. Koza, J. Stat. Phys. **85**, 179 (1996).
[13] M. Sinder and J. Pelleg, Phys. Rev. E **62**, 3340 (2000).
[14] S. Cornell, M. Droz, and B. Chopard, Phys. Rev. A **44**, 4826 (1991).
[15] S. Cornell and M. Droz, Phys. Rev. Lett. **70**, 3824 (1993).
[16] S. Cornell, Z. Koza, and M. Droz, Phys. Rev. E **52**, 3500 (1995).
[17] P. M. J. Trevelyan, D. E. Strier, and A. De Wit, Phys. Rev. E **78**, 026122 (2008).
[18] P. M. J. Trevelyan, Phys. Rev. E **79**, 016105 (2009).
[19] H. Taitelbaum, S. Havlin, J. E. Kiefer, B. Trus, and G. H. Weiss, J. Stat. Phys. **65**, 873 (1991).
[20] H. Taitelbaum, Yong-Eun Lee Koo, S. Havlin, R. Kopelman, and G. H. Weiss, Phys. Rev. A **46**, 2151 (1992).
[21] I. Hecht and H. Taitelbaum, Phys. Rev. E **74**, 012101 (2006).
[22] H. Taitelbaum and Z. Koza, Physica A **285**, 166 (2000).
[23] V. Malyutin, S. Rabinovich, and S. Havlin, Phys. Rev. E **56**, 708 (1997).
[24] P. V. Danckwerts, Trans. Faraday Soc. **46**, 701 (1950).
[25] H. S. Carslaw and J. C. Jaeger, *Conduction of Heat in Solids*, 2nd ed. (Clarendon, Oxford, 1959).
[26] J. Crank, *The Mathematics of Diffusion*, 2nd ed. (Oxford University Press, New York, 1975).
[27] B. Chopard, M. Droz, J. Magnin, and Z. Rácz, Phys. Rev. E **56**, 5343 (1997).
[28] J. Glimm and A. Jaffe, *Quantum Physics: A Functional Integral Point of View* (Springer, New York, 1981).
[29] MAPLE 8, Waterloo Maple Inc., Waterloo, Ontario, Canada, 2002.